Hindawi
Mathematical Problems in Engineering
Volume 2022, Article ID 7718400, 11 pages
https://doi.org/10.1155/2022/7718400

Research Article

Deconstruction of the Application of Police Drone Technology Integrating Fourier Fast Transform Algorithm in the 5G Network Era

Zhixue Zhang

Intelligent Police Equipment Lab of China People's Police University, Guangzhou, Guangdong 510663, China

Correspondence should be addressed to Zhixue Zhang; zhixue2002@163.com

Received 6 June 2022; Revised 28 July 2022; Accepted 3 August 2022; Published 25 August 2022

Academic Editor: Xiantao Jiang

In the era of the 5G network, the rapid development of information technology has made UAV technology widely used in many fields. UAVs have the characteristics of small size, lightweight, easy operation, flexibility, and so on. Drones can well solve the current problems of the insufficient police force, slow evidence collection, and harsh on-site environment. However, the existing police drones are often affected by objective conditions, such as the ground and weather when shooting, the signal is easily interrupted, and the accuracy and stability are not enough. In order to solve these problems, this article integrates the Fourier fast transform algorithm into the police unmanned aerial vehicle technology and improves the police unmanned aerial vehicle technology. By testing the police drones from four aspects of positioning and navigation, communication strength, shooting quality, and satisfaction, it can be observed how the police drones with the Fourier fast transform algorithm are optimized. Statistical experimental results show that the positioning and navigation accuracy of police drones has been improved. The communication strength command execution speed increased by 2.6%, the shooting quality increased by 6.7%, and the satisfaction rate increased by 7.3%. The Fourier fast transform algorithm makes police drones better, promotes the development of drone technology, and greatly improves the efficiency of police officers.

1. Introduction

A police drone is an unmanned aerial vehicle that has a power unit and a navigation module and is controlled to fly by a remote control device or automatically fly through a programmed route. The police drone aerial photography system uses drones to carry image acquisition equipment, takes advantage of the features of the 5G network, such as ultrahigh reliability, ultralow time extension, and ultralarge broadband, and transmits the captured images to the cloud without damage. Fourier fast transform algorithm is one of the most important algorithms in the field of signal processing and data analysis. Applying the Fourier fast transform algorithm to the police drone technology can capture the drone signal faster, transmit data, help the police handle official duties, and improve the efficiency of police dispatch.

The continuous popularization of UAV technology in various fields in the Internet era has led more scholars to invest in the research of UAV technology. Schilling proposed a vision algorithm to measure the orientation of a drone relative to the runway during landing. Firstly, the horizontal line was detected, and the boundary angle of the runway was recovered using the horizontal line information. From the horizon and boundary angles, pitch and bank angles could be determined. The range in which the yaw angle was located was also obtained [1]. Asatryan presented a method for UAV problem and state detection based on particle filter. Particle filters were applied to any state-space model, and the ability to handle nonlinear and non-Gaussian statistics made them suitable for drone problem detection. The experimental results showed that the detection method was more rapid and effective [2]. Renic

proposed a new concept of an intelligent combined UAV flight system. The system consists of multiple sub-UAVs. With multiple technologies, multishelf UAVs worked together to achieve mission perception, intelligent scene understanding, cluster control, integrated communication, ultralong battery life, and other functions [3]. Suzuki and Nonami investigated a layered finite element model for static structural analysis of CFRP laminate composites for unmanned aerial vehicle (UAV) wings. The nodules mimicked the protrusions on the leading edge of the pectoral fins of humpback whales and provided excellent performance from an aerodynamic standpoint. The nodular design of the leading edge of the UAV wing exhibited better performance, with a 38.75% reduction in deformation compared to normal [4]. Abdulrazaq et al. put forward a solution for drone GPS and INS navigation. The algorithm and process of the navigation system were developed, and a set of application programs and basic software systems were developed according to functional requirements. Simulation proved that using PID control and Kalman filter algorithm in the integrated navigation system could improve the accuracy of the navigation system [5]. Demuyakor studied improving attitude angle estimation during UAV landing based on a new horizon detection algorithm. By changing the mold to calculate the characteristic angle of the UAV, the simulation results were predictable. Camera installation restrictions were removed, and the calculation of UAV behavior information was simplified [6]. Anarase et al. discussed the basic principles and operation methods of UAV surveying and mapping technology. Taking the CX river water environment treatment project as an example, it was demonstrated that the UAV surveying and mapping technology had good application effect and research value in the classification research of various surveying and mapping elements and the comprehensive research on hierarchical surveying and mapping resources [7]. These studies demonstrate the beginnings of drone technology in various industries. But with the continuous development of the times, new problems have emerged.

Fast Fourier transform algorithms can locate signal frequencies and are used in many designs. Siran combined the wavelet transform with the Fourier fast transform algorithm, used the Fourier fast transform algorithm to calculate the discrete wavelet transform, and summarized the offset between the result and the filter length. The original signal could be completely reset by rotating the original rotation signal [8]. Townsend proposed a MATLAB Mho relay algorithm model based on the fast Fourier transform algorithm (FFT), modeled the power system, and simulated many fault conditions on selected transmission lines for evaluation. The results showed that, for each fault type, the relay worked normally in different positions [9]. Ibrahim and Shuaibu presented an improved Fourier-based fast transform algorithm to accurately measure harmonics and interharmonics. The algorithm used the frequency domain interpolation method to determine the fundamental frequency of the system, used the interpolation polynomial method to reconstruct the sampled time domain signal, and then used the Fourier fast transform algorithm to calculate the actual harmonic components. The results showed that the solutions determined by the proposed algorithm were more accurate and maintained reasonable computational efficiency [10]. Bakushinskii and Leonov proposed a new algorithm for computing the real discrete Fourier transform of even symmetric real-valued input sequences. By eliminating all unnecessary steps and storage locations, and by rearranging intermediate results and order of operations, the computation time and required core storage can be reduced by a factor of 2 compared to the case of arbitrary real inputs [11]. Bowman and Ghoggali aimed to solve the problem of denoising noisy ECG signals using fast Fourier transform-based bandpass filters. Multilevel adaptive peak detection was then applied to identify R peaks in the QRS complexes of the ECG signal. The test simulation results showed that the sensitivity and positive predictions were 99.98% and 99.96%, respectively. The accuracy and reliability of the proposed algorithm for detecting R peaks in ECG signals were confirmed [12]. Kuo et al. built a sound matching application using Ayat Al-Quran's pronunciation as a learning medium for children using FFT algorithms and divide-and-conquer methods that support independent learning. The tests were carried out, and the results showed that the accuracy of correct readings was 61.1%, and the accuracy of false readings was 38.9% [13]. Khayyeri and Mohammadi introduced the MATLAB simulation model of a smart meter for energy balance analysis based on FFT algorithm, which can calculate accurate power parameters. Comparing the results of the FFT analysis function of the MATLAB software Powergui module with the simulation model, the correctness of the method was verified [14]. These studies show that the Fourier fast transform algorithm has a boosting effect on many industries, but it is less used in drones.

In this article, the Fourier fast transform algorithm is integrated into the application of police UAV technology in the era of the 5G network. The 5G network will endow networked drones with important capabilities such as real-time ultrahigh-definition image transmission, and long-distance low-latency control. The Fourier fast transform algorithm reconstructs the original spectrum of the signal efficiently and with high probability using some sampling points. It can analyze the frequency data of the UAV to implement precise positioning and optimize the technology of the police UAV.

2. Optimization Process of Police Drones

2.1. 5G Network-Connected Police UAV Data Transmission and Control. 5G network provides general network solutions from wireless to central network to adapt to network applications in many complex application scenarios. After both the drone terminal and the 5G ground control terminal connected to the drone network transmit control data and processes through the 5G network, multiple scenarios are transmitted through the network server. The new 5G optical projection has multiple technologies, such as multiple-input multiple-output (MIMO) technology, beamforming technology, new spectrum, scalable waveform based on OFDM,

new flexible design based on low-latency slot structure, and 5G network slicing technology, with a specific process as shown in Figure 1 [15].

Current networks face the problem of power requirements and finding field sources. This can be solved with 5G Multiple Input Antenna (MIMO) solutions. MIMO (multiple input/multiple output) is a technology used to increase the speed and quality of wireless data transmission. Multiple antennas are used to transmit and receive different data and increase the capacity of multiple networks. In commercial networks, antennas are often compatible with drones and ground terminals operating at high altitudes to improve transmission signals, reduce complex field interference and up and down interference, and improve the ground [16].

2.2. Hardware Requirements for Police Drones. The overall requirements of the hardware system of the police UAV are shown in Figure 2. It is roughly composed of these parts: rack, battery, motor, ESC, flight control, image transmission, data transmission, photoelectric pod (gimbal camera), sensor, ground station, and remote control.

2.2.1. Drone Rack. The racks are the backbone of each drone rotor, providing support and mounting locations for the remaining components, as well as improving specific collision avoidance properties. In the event of a collision, it avoids damage to the rest of the components, installs it reasonably, and can easily fold the drone for easier portability.

2.2.2. Battery. The battery powers the whole system, the rotation of the motor powers the drone, and the rotating motor is mainly controlled by an ESC, also called a motor governor. It allows the flight control aircraft to receive the control of the motor through the flight control algorithm and can also output a pulse frequency modulation (PWM) signal that controls the actual motor performance.

2.2.3. Flight Control Board. The aircraft control panel is the main component of the drone. It is the center of a drone by accepting ground commands and then completing daily tasks such as sensor data loading, behavioral data analysis, and log information recording in the operating environment. The performance of the flight control board is related to the quality of the entire drone.

2.2.4. Image Transmission. The image transmission first sends the image information received by the PTZ camera to the ground station through certain wireless devices such as antennas so that the ground observer can detect the position of the power line in real time. The relevant behavior data and GPS data captured by the UAV and the information of each component of the UAV can be provided to the user through the ground station sensor for data analysis and local data storage. The overall flight status of the UAV rotor is determined through the data [17].

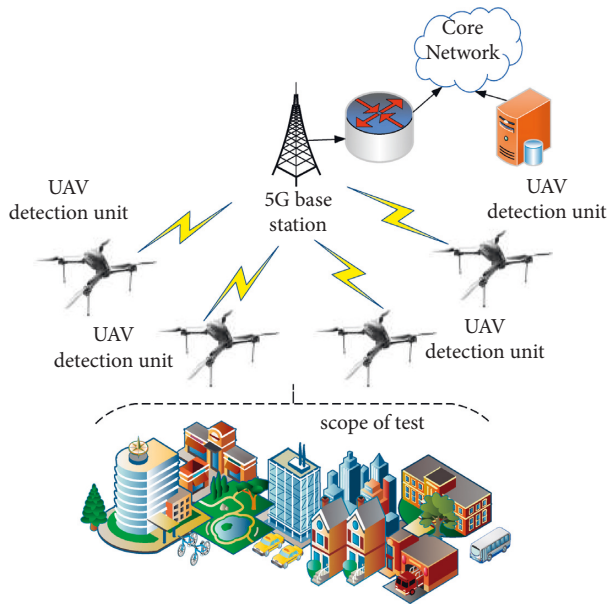

Figure 1: Data transmission and control of 5G network-connected police drones.

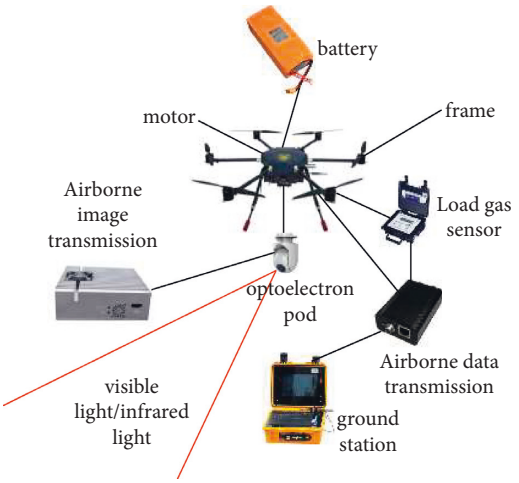

Figure 2: Hardware requirements for police drones.

2.2.5. PTZ Camera. The gimbal camera is used to capture the pictures seen by the drone and transmit them to the user. Since the drone is easily affected by the wind when it flies to a high altitude, the captured pictures are shaken violently, and key information cannot be accurately obtained. Each drone consists of a gimbal and a camera. The gimbal can stabilize the drone shooting equipment very well, and when there are external factors, it can still deliver a clear picture to the user.

2.2.6. Sensors. The sensor firstly obtains the relevant information of the UAV and sends it to the aircraft control panel to calculate the behavior and position of the UAV and then calculate the flight speed to ensure the stability of the UAV. The remote control is a sensor, which is used to control the flight of the drone and the shooting of the gimbal camera and transmits the data from the remote control to

the aircraft controller for calculation. But under close control, the data recorded by the sensor is the real value, and the remote data is the expected value.

2.2.7. Ground Station. There are two antennas in the ground station for image transmission and data transmission. At the same time, the ground station system provides an application interface for displaying the collected data and supports local storage of the data. It makes it easier for users to discover more details about police drones and video captured by cameras [17, 18].

3. Fast Fourier Transform Calculation Mathematical Model

3.1. Fourier Series. There are two expressions for the Fourier series: trigonometric functions and exponential complex numbers; trigonometric functions are periodic functions represented by the sum of a series of trigonometric functions, sine and cosine [19]. For example,

$$f(a) = \begin{cases} 0 & -\pi \le x \le 0, \\ 1 & 0 \le x \le \pi, \end{cases} \tag{1}$$

$f(a)$ is extended to $g(a)$with a period of 2π, and the Fourier series corresponding to $g(a)$is as follows:

$$\begin{aligned} g(a) &= \frac{1}{2} + \frac{2}{\pi}\left[\sin x + \frac{\sin 3x}{3} + \frac{\sin 5x}{5} + \dots\right] \\ &= \frac{1}{2} + \sum_{m=1}^{\infty} \frac{1}{m\pi}\left[1 - (-1)^m\right] \sin mx. \end{aligned} \tag{2}$$

Formula (2) shows that a periodic signal at any given time can be converted into a series of sine and cosine signals with varying amplitudes, no matter how large. The specific expression is as follows:

$$x(a) = \frac{b_0}{2} + \sum_{m=1}^{\infty} X_i\left(b_k \cos k\Omega_0 a + c_k \cos k\Omega_0 a\right), \tag{3}$$

where b_0 is the static variable, the DC component of the signal, and c_k are the sinusoidal signal and the amplitude of the sinusoidal signal, respectively, and $k\Omega 0$ is the frequency of the signal.

Although the triangular shape of the Fourier series is very clear, the expression is very complex and often consists of three parts. The first part is the sine-cosine expression of the function, the second part is the coefficients of the function, and the third part is a constant. There is a certain difficulty in writing and drawing. However, complex expressions for the Fourier series can solve these problems.

Euler's formula can combine sines and cosines of the same frequency in pairs, namely,

$$e^{z\Omega} = \cos \Omega + z \sin \Omega. \tag{4}$$

Multiplying all the sine by the factor "z," the sine function and the coefficient of the sine function are obtained by combining the trigonometric functions:

$$\left|B_k = \sqrt{b_k^2 + c_k^2}\right|. \tag{5}$$

The complex exponential expression is obtained:

$$x(a) = b_0 + \sum_{k=1}^{\infty} B_k e^{zk\Omega_0 a}. \tag{6}$$

3.1.1. Fourier Series Expansion of Square Wave Signal

$$\begin{aligned} f(a) &= \frac{4b}{\pi^2}\sin\left(2\pi f_0 a\right) + \frac{4b}{3\pi^2}\sin\left(6\pi f_0 a\right) \\ &\quad + \frac{4b}{5\pi^2}\sin\left(10\pi f_0 a\right) + \dots. \end{aligned} \tag{7}$$

Formula (7) shows that the odd and high-frequency bands are grouped according to their respective dimensions to form a square wave signal with almost constant magnitude. The frequency range of each instruction of the rectangular wave signal calculated by the Fourier series varies with the original sampling method, but the signal amplitude remains unchanged, and the frequency of each instruction remains unchanged [20].

3.1.2. Fourier Series Expansion of Triangular Wave Signal

$$\begin{aligned} f(a) &= \frac{8b}{\pi^2}\sin\left(2\pi f_0 a\right) + \frac{8b}{9\pi^2}\sin\left(2\pi f_0 a\right) \\ &\quad + \frac{8b}{25\pi^2}\sin\left(2\pi f_0 a\right) + \dots. \end{aligned} \tag{8}$$

Formula (8) shows that the odd and high-frequency bands are grouped according to their respective dimensions to form a triangular wave signal. The size is almost negligible. The frequency range of each instruction of the triangular wave signal calculated by the Fourier series varies with the original sampling method, but the signal amplitude remains unchanged, and the frequency of each instruction remains unchanged [21].

3.2. DFT Spectrum Analysis. The discrete Fourier transform is called DFT for short. DFT spectral division indicates a new discrete sampling direction at the endpoints of the Fourier sequence and allows digital signal processing to be successfully implemented digitally in frequency mode. It enables the efficient application of digital signal processing to police drone technology and is the main tool of modern signal spectrum analysis [22].

The definition of continuous Fourier transform is as follows:

$$F(k\Delta f) = \int_{-\infty}^{\infty} f(m\Delta a) e^{-z2\pi k\Delta f m\Delta t} da. \tag{9}$$

The integrals are turned into sums, resulting in the following:

$$X(k\Delta f) = \sum_{m=0}^{N-1} x(m\Delta a)e^{-z2\pi k f_s/Nm1/f_s}\Delta a. \tag{10}$$

The N-point time domain truncation is performed as follows:

$$\begin{aligned} X(k\Delta f) &= \sum_{m=0}^{N-1} x(m\Delta a)e^{-z2\pi k f_s/Nm1/f_s}\Delta a \\ &= \sum_{m=0}^{N-1} x(m\Delta a)e^{-z2\pi/Nkm}\Delta m. \end{aligned} \tag{11}$$

Since $x(m\Delta a)$ and $X(k\Delta f)$ are the time function value $x(m)$ of the mth point after discretization and the Fourier transform value $X(k)$ of the kth point, the DFT is defined as follows:

$$\begin{aligned} X(k) &= \sum_{m=0}^{N=1} x(m\Delta a)e^{-z\frac{2\pi}{N}} \\ &= \sum_{M=0}^{M-1} x(m)\left[\cos\left(\frac{2\pi}{M}km\right)\right], k = 0, 1, \ldots, M-1. \end{aligned} \tag{12}$$

In the formula, k is the serial number of the discrete spectral line, N is the length of the time series, and the real and imaginary parts of the discrete Fourier transform are as follows:

$$X_R = \sum_{m=0}^{M-1} x(m)\cos(2\pi/Mkm), k = 0, 1, 2, \ldots M-1, \tag{13}$$

$$X_I = \sum_{m=0}^{M-1} x(m)\sin\left(\frac{2\pi}{M}km\right), k = 0, 1, 2, \ldots, M-1. \tag{14}$$

After the periodic signal has undergone DFT, several parameters of the signal can be derived from the formula. These are the magnitude, spectrum, power spectrum, log spectrum, and phase spectrum, respectively.

3.3. Fast Fourier Transform. Fast Fourier Transform is abbreviated as FFT. Its purpose is to assign a unique Fourier transform rate to each length in the short-term DFT algorithm. When M is an even number, the DFT of M points is equal to the DFT of $N/2$ points [12, 23].

Take the sequence of M $x(n)$, $n = 0, 1, \ldots, M-1$ according to even and odd sequences of length $M/2$ (subtracted over time) [24]:

$$\begin{cases} x_1(r) = x(2r) \\ x_{21}(r) = x(2r+1) \end{cases} r = 0, 1, \ldots, M/2-1. \tag{15}$$

According to formula (15), $W_M^2 = W_{M/2}$; the DFT of the sequence $x(m)$ can be expressed as follows:

$$\begin{aligned} X(k) = DFT[x(m)] &= \sum_{m=0}^{M-1} x(m)W_M^{mk} = \sum_{\substack{m=0 \\ m\,is\,even}}^{M-1} x(m)W_M^{mk} + \sum_{\substack{m=0 \\ m\,is\,odd}}^{M-1} x(m)W_M^{mk} \\ &= \sum_{r=0}^{M/2-1} x(2r)W_{M/2}^{rk} + \sum_{r=0}^{M/2-1} x(2r+1)W_{M/2}^{(2r+1)k} = \sum_{r=0}^{M/2-1} x_1(r)W_{M/2}^{rk} + W_M^k \sum_{r=0}^{M/2-1} x_2(r)W_{M/2}^{rk} \\ &= X_1(k) + W_M^k X_2(k), k = 0, 1, \ldots, N/2-1. \end{aligned} \tag{16}$$

Formula (16) shows that the DFT of point M is decomposed into the DFT of $M/2$ points, and the DFT of 2 points M can be combined into one DFT.

That is, the column length of $x1(r)$ and $x2(r)$ is $M/2$, and the number of points of their DFTX1 (k) and $X2$ (k) is also $M/2$. And $x(m)$ has M points, then the second half value of $X(k)$ $(M/2 = k = M-\text{-}1)$ is given as follows:

$$\begin{aligned} X\left(\frac{k+M}{2}\right) &= X_1\left(\frac{k+M}{2}\right) + W_M^{(k+m/2)} \bullet X_2\left(\frac{k+M}{2}\right), \\ &0 \frac{\leq k \leq M}{2} - 1. \end{aligned} \tag{17}$$

The periodicity of the coefficients is applied to get $W_{M/2}^{r(k+M/2)} = W_{M/2}^{rk}$. It can be pushed out as follows:

$$\begin{aligned} X_1\left(\frac{k+M}{2}\right) &= \sum_{r=0}^{M/2-1} x_1(r)W_{M/2}^{r(k+M/2)} \\ &= \sum_{r=0}^{M/2-1} x_1(r)W_{M/2}^{rk} = X_1(k). \end{aligned} \tag{18}$$

Formula (18) yields $X2(k + M/2) = X2(k)$. At the same time, it is shown that $X1(k)$ and $X2(k)$ obtained by half of k values $(M/2 = k = m\text{ - }1)$ are equal to $X1(k)$ and $X2(k)$ corresponding to the first half of K values $(0 = k = M/2-1)$. Then according to $WE(k + MZ2) = -W$, the DFTX(k) corresponding to N points can be calculated by these two formulas:

$$\begin{cases} X(k) = X_1(k) + W_M^k X_2 \\ X\left(\dfrac{k+M}{2}\right) = X_1(k) - W_M^k X_2(k) \end{cases} \quad 0 \le k \le M/2 - 1. \tag{19}$$

Formula (19) computes all values $X(k)$ from the first 0 to $X(k)$. The factorial factor W_M^k in the formula plays a role in the multiplication of complex numbers and is called the rotation factor [25, 26].

4. Optimal Experimental Design of UAV Technology

4.1. Experimental Process. In order to optimize the existing UAV technology, this article proposes to introduce the Fourier fast transform algorithm into the police UAV technology in the era of the 5G network. In order to prove the optimization effect of the Fourier transform algorithm on the police drone technology, experiments are carried out, and three traditional police drones are selected and named drone 1, drone 2, and drone 3. The police UAV incorporating the Fourier fast transform algorithm is named drone 4, and the four drones are tested in four aspects: positioning and navigation, communication strength, shooting image quality, and satisfaction test. In order to avoid experimental errors, the hardware assembly of the four drones is the same and tested in the same environment. After the test is over, the test results are counted and analyzed.

4.2. Experimental Data. The detailed data of the selected four police drones are shown in Table 1.

4.3. The Purpose of the Experiment. The optimization effect of the Fourier fast transform algorithm on police drone technology is tested. What improvements are made in different aspects and how much it is improved will be proved by experiments.

5. Influence Results of Fusion Fourier Fast Transform Algorithm on UAV Technology

5.1. Positioning and Navigation Test. Positioning and navigation are important functions of police drones. The four drones were tested for positioning and navigation. The test locations were urban and suburban areas to observe whether the drones could reach the designated location. In order to ensure the accuracy of the experiment, each drone was tested for positioning and navigation accuracy 5 times, and the test sites were separated by 100 meters, 300 meters, 500 meters, 700 meters, and 1000 meters from the starting point. The test results are shown in Figure 3.

Figure 3(a) is the test result in the urban area, and Figure 3(b) is the test result in the suburban area. As the test distance increases, the unfavorable factors that appear during the flight of the drones are also increasing, resulting in the increasing error distance of the drones. The experimental results show that the accuracy of drone 4 is higher than that of drone 1, drone 2, and drone 3, regardless of whether the test site is in the urban area or the suburbs. In the drone positioning and navigation test results in the urban area, it is found that the sum of the five test error results of drone 1 is 36.4 meters, the sum of the five test error results of drone 2 is 36.3 meters, and the five test results of drone 3 are 36.3 meters. The sum of the test error results is 37 meters, and the sum of the five test error results of drone 4 is 34.1 meters. In the results of the UAV positioning and navigation test results in the suburbs, it is found that the sum of the five test error results of drone 1 is 39.3 meters, the sum of the five test results of drone 2 is 39.4 meters, and the five test results of drone 3 are 39.4 meters. The sum of the error results is 39.8 meters, and the sum of the error results of the five tests of drone 4 is 36.7 meters. To sum up, the suburban environment is complex and there are many obstructions, and the error distance of drone positioning and navigation in the suburbs is greater than the error distance of drone positioning and navigation in the urban area. The average error distance of the traditional police drone is 38.03 meters, and the average error distance of the police drone integrated with the Fourier fast transform algorithm is 35.4 meters, and the accuracy is increased by 6.9%. The Fourier fast transform algorithm can better perform positioning calculations and help police drones reach their destinations accurately.

5.2. Communication Strength. The police drone needs to transmit the specific situation of the execution site in time, and the strength of the communication strength affects the speed of the police drone to execute the remote control command and the speed of uploading the captured image. Four drones were tested for communication strength. To avoid experimental errors, the image transmission frequency band is uniformly set to 1.4 GHz. It tests the command execution speed and the image upload speed indoors and outdoors, respectively. The test results are shown in Figure 4.

Figure 4(a) is the result of the command execution speed test, and Figure 4(b) is the result of the image upload speed test. The experimental results show that the command execution speed and image upload speed of drone 4 are higher than those of drone 1, drone 2, and drone 3, regardless of whether the test site is indoors or outdoors. The indoor environment is quiet and there are few interference factors, and the command execution speed and image upload speed of the drone are higher than those in the outdoor. In the instruction execution speed diagram of Figure 4(a), the execution response time of drone 4 is slightly lower than that of drone 1, drone 2, and drone 3. The average execution speed of instructions in the traditional police drone indoors is 1.313 seconds. The average speed of instruction execution outdoors is 2.206 seconds. In Figure 4(b), the uploading speed of drone 4 is lower than that of drone 1, drone 2, and drone 3. The average upload time of traditional police drone indoors is 6.26 seconds. The average image upload time outdoors is 10.51 seconds. To sum up, the average command execution speed of traditional police drones is 1.76 seconds, and the average command execution speed of police drones incorporating the Fourier fast transform algorithm is 1.715

Table 1: Experimental data.

	Weight (g)	Battery capacity (mAh)	Initial flight speed (m/s)	Maximum takeoff altitude (m)	Usage time (day)
Drone 1	595	3500	6	4000	298
Drone 2	596	3500	6	4000	290
Drone 3	595	3500	6	4000	315
Drone 4	596	3500	6	4000	317

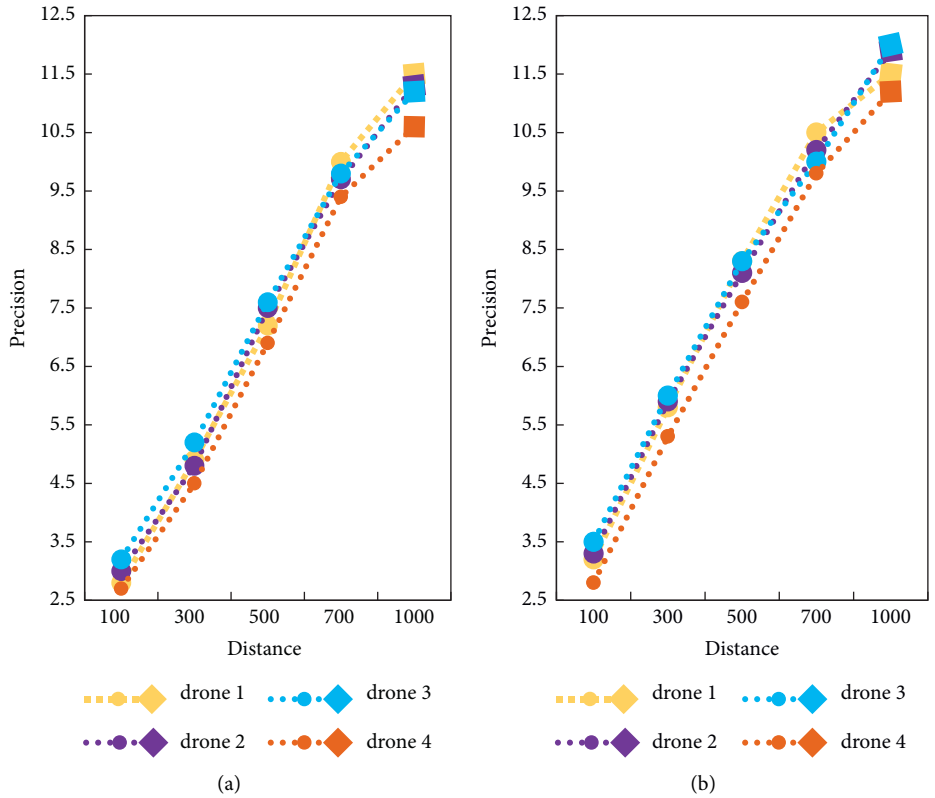

Figure 3: Positioning and navigation test. (a) Urban test results; (b) suburban test results.

seconds, with a speed increase of 2.6%. The average image upload speed of traditional police drones is 8.385 seconds, and the average image upload speed of police drones incorporating the Fourier fast transform algorithm is 8.31 seconds, with an increase of 0.8%. The image upload speed increase is small, and the test environment cannot be kept completely consistent, which can be ignored.

5.3. Shooting Quality. The quality of the shooting image affects the final shooting result. The clear image quality allows the police to understand the details of the shooting location and improve work efficiency. The test time periods for shooting image quality are 8:00 to 9:00 in the morning, 11:30 to 12:30 in the afternoon, 15:00 to 1600 in the afternoon, and 19:00 to 20:00 in the evening. The filming time is 1 minute, and 5 locations are randomly selected for filming, named location 1, location 2, location 3, location 4, and location 5.

Figure 5(a) is the test result from 800 to 9:00, Figure 5(b) is the test result from 11:30 to 12:30, and Figure 5(c) is the test result from 15:00 to 16:00. Figure 5(d) is the test results from 19:00 to 20:00. It can be seen from Figure 5 that the shooting quality parameters are relatively high from 8:00 to 9:00 in the morning and from 15:00 to 16:00 in the afternoon, slightly lower at noon due to the influence of sunlight, and the lowest at night due to the dark environment. In Figure 5(a), the average image quality parameter of the traditional police drone shot is 105.3, and the average image quality parameter of the police drone shot with the Fourier fast transform algorithm is 110.4. In Figure 5(b), the average image quality parameter of the traditional police drone shot is 94.93, and the average image quality parameter of the police drone shot with the Fourier fast transform algorithm is 99.4. In Figure 5(c), the average image quality parameter of the traditional police drone shot is 105.47, and the average image quality parameter of the police drone shot with the Fourier fast transform algorithm is 112.4. In Figure 5(d), the average image quality parameter of the traditional police drone shot is 68.47, and the average image quality parameter of the police drone shot with the Fourier fast transform algorithm is 77. To sum up, the average image quality

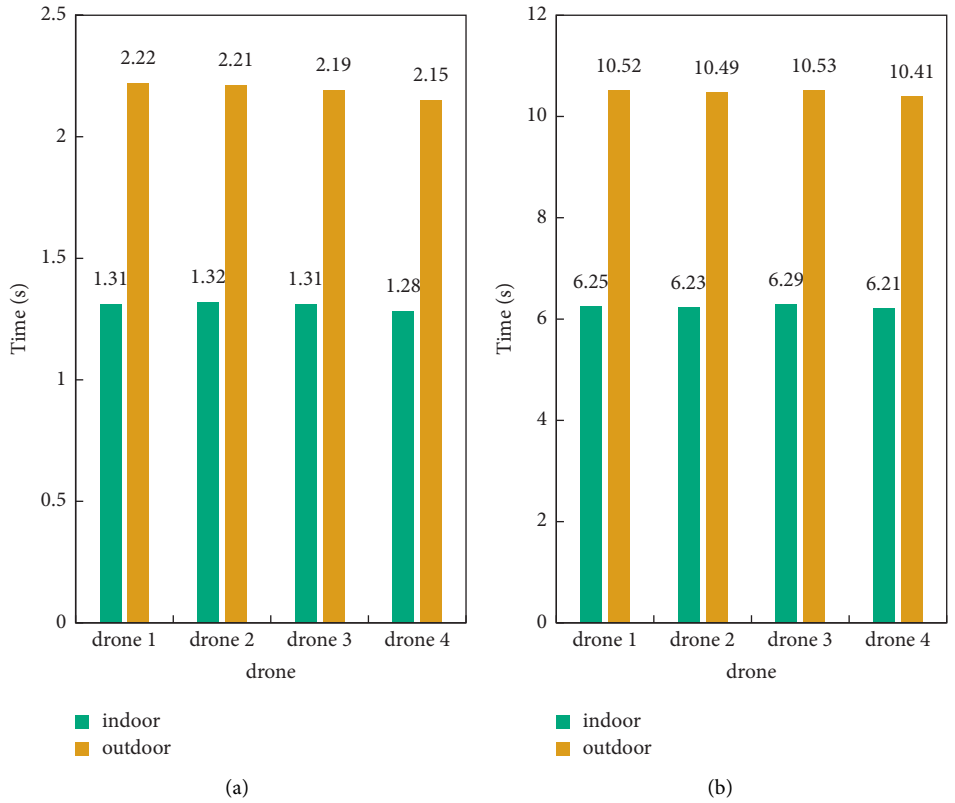

Figure 4: Communication strength test. (a) Command execution speed; (b) image upload speed.

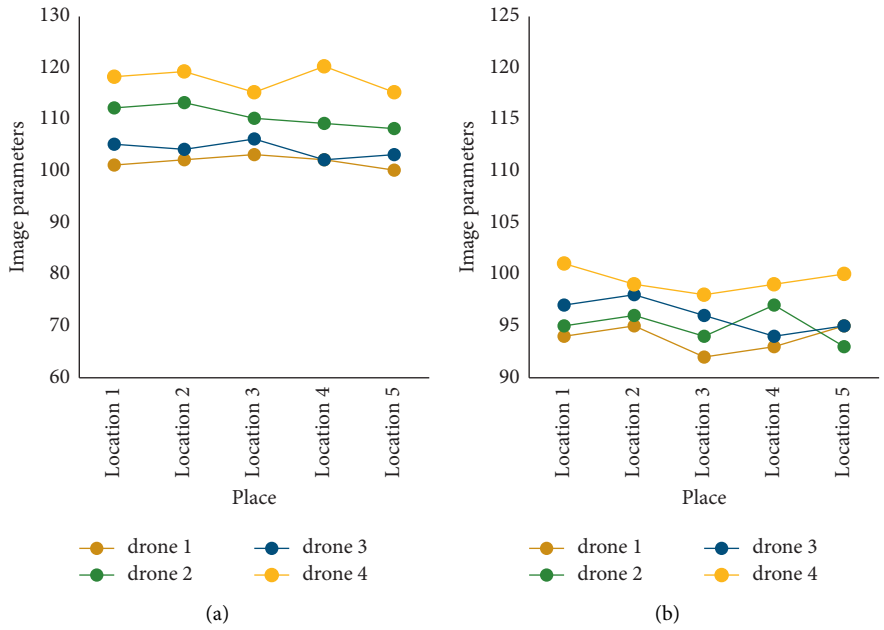

Figure 5: Continued.

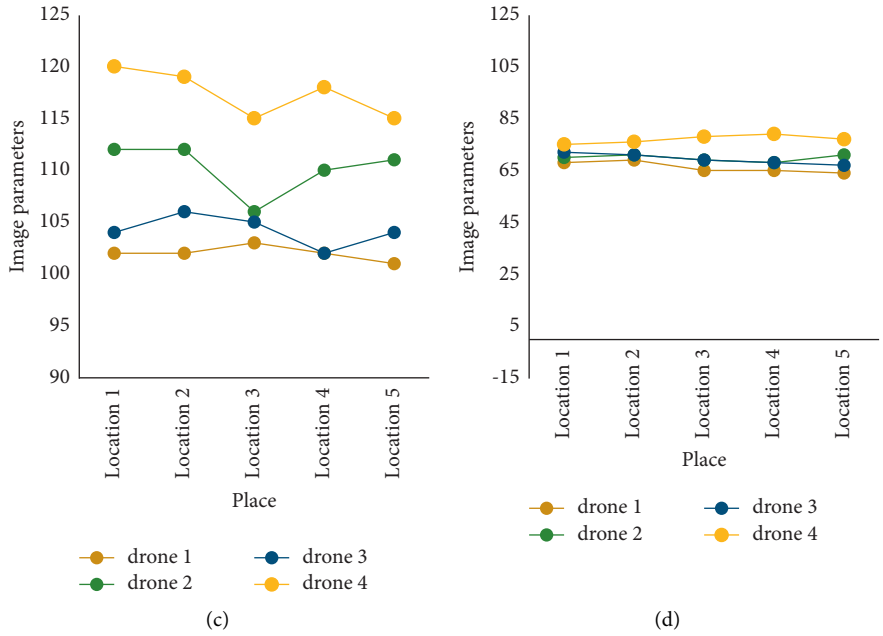

Figure 5: Shooting quality test. (a) 8:00 to 9:00; (b) 11:30 to 12:30; (c) 15:00 to 16:00; (d) 19:00 to 20:00.

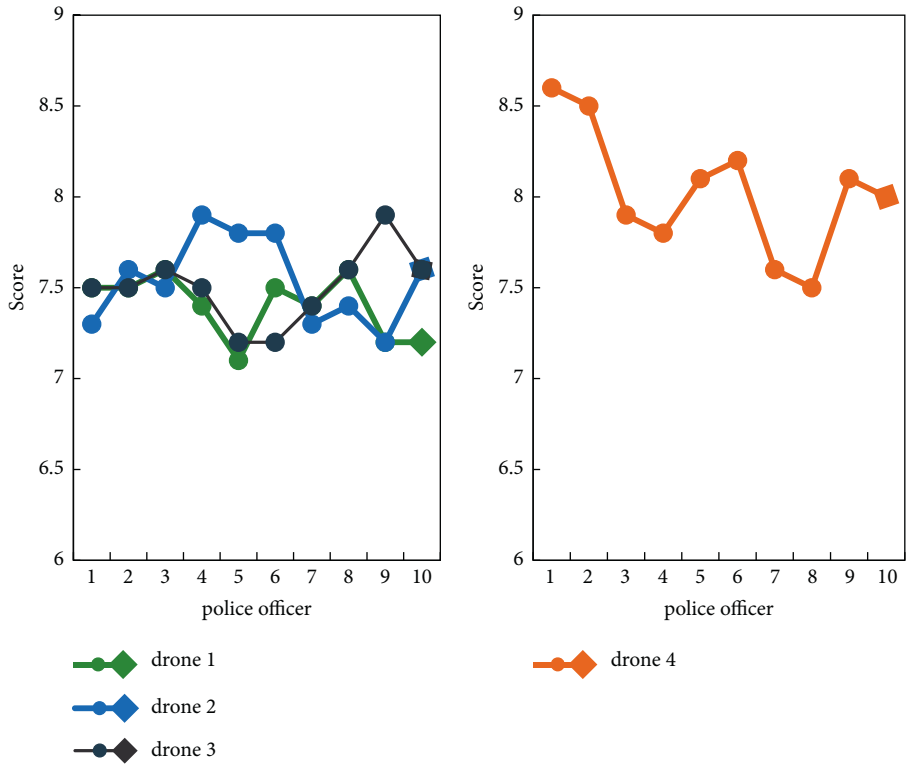

Figure 6: Test of satisfaction.

parameter of traditional police drones in different time periods is 93.54. The average image quality parameter of the police drone integrated with the Fourier transform algorithm in different time periods is 99.8, and the shooting image quality is improved by 6.7%.

5.4. Satisfaction Test. Ten police officers are randomly selected to operate drone 1, drone 2, drone 3, and drone 4. After the operation is completed, different drones are scored, with a full score of 10. The specific results are shown in Figure 6.

The figure shows that the score of drone 4 is significantly higher than that of drone 1, drone 2, and drone 3. Drone 1 has an average satisfaction rating of 7.4. Drone 2 has an average satisfaction rating of 7.54. Drone 3 has an average satisfaction rating of 7.5, and drone 4 has an average satisfaction rating of 8.03. The average satisfaction score of the traditional police drone is 7.48, and the average satisfaction score of the police drone integrated with the Fourier fast transform algorithm is 8.03, with a 7.3% increase in satisfaction. To sum up, the police drone incorporating the Fourier fast transform algorithm is more satisfactory to the users than the traditional police drone.

6. Conclusion

Police drones can greatly improve the efficiency of police officers. Through police drones, they can understand the scene at the first time, make analysis, and take the next action in time. The improvement of police drone technology will change very necessary. In this article, the Fourier fast transform algorithm was integrated into the police drone technology in the 5G network era and was studied. The Fourier fast transform algorithm makes the positioning function of UAV technology more accurate. The drone can reach a specified location accurately, and the communication strength is also greatly improved compared with the traditional police drone. Whether it is indoors or outdoors, the drone can execute quickly after receiving instructions. DFT spectrum analysis makes the shooting quality of the drone clearer. It can still transmit high-quality video and pictures under strong light and dark shooting conditions. Through a satisfactory survey of users, it is found that based on Fourier fast transform algorithm, police drone technology is more popular with users. The addition of the Fourier fast transform algorithm greatly optimizes the UAV technology and promotes the development of the UAV industry. The addition of the Fourier fast transform algorithm greatly optimizes the UAV technology and has greatly promoted the development of UAV technology.

Data Availability

The data used to support the findings of this study are available from the corresponding author upon request.

Conflicts of Interest

The authors declare no conflicts of interest.

References

[1] R. Schilling, P. Kleinschmidt, and J. Borger, "Using drone technology to minimize socioeconomic and ethnic cardiac arrest survival disparities within North Carolina," *North Carolina Medical Journal*, vol. 80, no. 6, pp. 381-382, 2019.

[2] G. Asatryan and J. Kalpakian, "Book review of the drone age: how drone technology will change war and peace: by Michael J. Boyle, Oxford University Press," *Critical Studies on Terrorism*, vol. 14, no. 3, pp. 1–3, 2021.

[3] N. C. Renic, "The drone age: how drone technology will change war and peace. By michael J. Boyle. Oxford: oxford university press, 2020. 400p. $29.95 cloth," *Perspectives on Politics*, vol. 19, no. 3, pp. 958-959, 2021.

[4] S. Suzuki and K. Nonami, "Special issue on novel technology of autonomous drone," *Journal of Robotics and Mechatronics*, vol. 33, no. 2, p. 195, 2021.

[5] A. Abdulrazaq, H. Zuhriyah, and N. A. Istiqomah, "Toward A novel design for spray disinfection system to combat coronavirus (Covid-19) using IoT based drone technology[J]," *Revista Argentina de Clinica Psicologica*, vol. 29, no. 5, pp. 240–247, 2020.

[6] J. Demuyakor, "Ghana go digital agenda: the impact of zipline drone technology on digital emergency health delivery in Ghana," *Shanlax International Journal of Arts, Science and Humanities*, vol. 8, no. 1, pp. 242–253, 2020.

[7] M. S. Anarase, G. K. Sasane, S. A. Dhenge, S. D. Gorantiwar, P. A. Ghadage, and R. B. Kalamkar, "Training need of MPKV ph.D. Students towards application of drone technology in agriculture," *International Journal of Current Microbiology and Applied Sciences*, vol. 9, no. 9, pp. 3443–3448, 2020.

[8] W. Wang, Z. Li, J. Wu, and Z. Wang, "Accelerated near-field algorithm of sparse apertures by non-uniform fast Fourier transform," *Optics Express*, vol. 27, no. 14, pp. 19102–19118, 2019.

[9] A. Townsend, "Nonuniform fast fourier transform based on low rank approximation[J]," *SIAM Journal on Scientific Computing*, vol. 40, no. 1, pp. A529–A547, 2018.

[10] M. Ibrahim and Z. Shuaibu, "Enhancement of retinex algorithm using fast fourier transform," *International Journal of Computer Application*, vol. 177, no. 18, pp. 26–31, 2019.

[11] A. B. Bakushinskii and A. S. Leonov, "Fast solution algorithm for a three-dimensional inverse multifrequency problem of scalar acoustics with data in a cylindrical domain," *Computational Mathematics and Mathematical Physics*, vol. 62, no. 2, pp. 287–301, 2022.

[12] J. C. Bowman and Z. Ghoggali, "The partial fast fourier transform," *Journal of Scientific Computing*, vol. 76, no. 3, pp. 1578–1593, 2018.

[13] C. C. Kuo, H. C. Chuang, A. H. Liao et al., "Fast Fourier transform combined with phase leading compensator for respiratory motion compensation system," *Quantitative Imaging in Medicine and Surgery*, vol. 10, no. 5, pp. 907–920, 2020.

[14] M. Khayyeri and K. Mohammadi, "Cooperative wideband spectrum sensing in cognitive radio based on sparse real valued fast Fourier transform," *IET Communications*, vol. 14, no. 8, pp. 1340–1348, 2020.

[15] A. Diet, C. Berland, M. Villegas, and G. Baudoin, "EER architecture specifications for OFDM transmitter using a class E amplifier," *IEEE Microwave and Wireless Components Letters*, vol. 14, no. 8, pp. 389–391, 2004.

[16] Q. M. Ha, Y. Deville, Q. D. Pham, and M. H. Hà, "On the min-cost traveling salesman problem with drone," *Transportation Research Part C: Emerging Technologies*, vol. 86, no. 7, pp. 597–621, 2018.

[17] H. Goh, "Analysis of static and dynamic efficiency for sustainable growth of Edu-tech companies," *Journal of Logistics, Informatics and Service Science*, vol. 7, no. 1, pp. 87–101, 2020.

[18] E. Komagal and B. Yogameena, "Correction to: foreground segmentation with PTZ camera: a survey," *Multimedia Tools and Applications*, vol. 81, no. 5, pp. 7523–7526, 2022.

[19] S. Vagheesan∗ and J. Govindarajulu, "Comparative regression and neural network modeling of roughness and kerf width in

CO2 laser cutting of aluminium," *Tehnički Vjesnik*, vol. 28, no. 5, pp. 1437–1441, 2021.

[20] D. Chowdhury, P. Gharami, and J. Akter, "Implementing advanced software in construction project management and control," *Journal of Logistics, Informatics and Service Science*, vol. 6, no. 1, pp. 87–105, 2019.

[21] Y. Jiang, S. Liu, and X. Wu, "Online identification of the rotor flux linkage in permanent magnet synchronous motors with position triangular signal injection[J]," *Zhongguo Dianji Gongcheng Xuebao/Proceedings of the Chinese Society of Electrical Engineering*, vol. 39, no. 3, pp. 845–856, 2019.

[22] X. Wang, S. Hu, E. Wang, Q. Zhang, and B. Liu, "Extraction of vibration waveform characteristics of dry ice powder pneumatic rock breaking using Hilbert-Huang transform," *Arabian Journal of Geosciences*, vol. 15, no. 1, pp. 71–15, 2022.

[23] L. Liu, T. Chen, S. Gao, Y. Liu, S. Yang, and X. Wang, "Optimization of agricultural machinery allocation in heilongjiang reclamation area based on particle swarm optimization algorithm," *Tehnički Vjesnik*, vol. 28, no. 6, pp. 1885–1893, 2021.

[24] D. Ruiz-Antolín and A. Townsend, "A nonuniform fast fourier transform based on low rank approximation," *SIAM Journal on Scientific Computing*, vol. 40, no. 1, pp. A529–A547, 2018.

[25] A. Beauducel and M. Kersting, "Identification of facet models by means of factor rotation: a simulation study and data analysis of a test for the berlin model of intelligence structure," *Educational and Psychological Measurement*, vol. 80, no. 5, pp. 995–1019, 2020.

[26] W. Kinlaw, M. Kritzman, and D. Turkington, "Practical applications of crowded trades: *Implications for sector Rotation and factor timing*," *Practical Applications*, vol. 8, no. 1, pp. 5-6, 2020.